

# Interfacial Structure of Poly(methyl methacrylate)/TiO<sub>2</sub> Nanocomposites Prepared Through Photocatalytic Polymerization

Jiao Wang, Xiuyuan Ni

*The Key Laboratory of Molecular Engineering of Polymers, Department of Macromolecular Science, Ministry of Education, Shanghai 200433, China*

Received 16 July 2007; accepted 29 December 2007

DOI 10.1002/app.28020

Published online 6 March 2008 in Wiley InterScience (www.interscience.wiley.com).

**ABSTRACT:** Poly(methyl methacrylate)/TiO<sub>2</sub> nanocomposites have been prepared by the polymerization with photoexcited TiO<sub>2</sub> nanoparticles as initiator. To reveal the interfacial structure, the composites obtained are investigated by FTIR and XPS analysis. The bound PMMA displays triply split IR bands attributed to the carbonyl stretching mode, meanwhile great changes also occur in the IR range closely related to the conformation of PMMA. Based on the area of the nonassociated and associated PMMA carbonyl stretching peaks in the FTIR spectrum, it is calculated out that the bound PMMA is constituted of 70% repeating units in non-associated state and 30% units associated to TiO<sub>2</sub> inorganic nanoparticles. Moreover, XPS analysis show that Ti2p dou-

blet of the composites shift to lower binding energy by 1.0 eV, indicating the interaction between Ti atoms of TiO<sub>2</sub> and oxygen atoms of PMMA. According to the observation that the interaction involves both carboxyl and carbonyl groups of PMMA, a bidentate complex is approved. In addition, compared with the extracted PMMA, certain backbone chains of bound PMMA have to change their rotational conformations from gauche to trans so as to bond to the surface active centers at TiO<sub>2</sub> nanoparticles. © 2008 Wiley Periodicals, Inc. *J Appl Polym Sci* 108: 3552–3558, 2008

**Key words:** poly(methyl methacrylate); TiO<sub>2</sub>; photopolymerization; Interface; FTIR; XPS

## INTRODUCTION

The composites of polymers and inorganic nanoparticles have been usually prepared by means of mixing and in-situ polymerization. In the in-situ polymerization, the monomers are initiated by the organic initiators that have been located on the nanoparticles' surface in advance.<sup>1</sup> It is well known that the UV-excitation of semiconductors produces valence hole and conduction electron in pairs, which catalyze reactions on the surface.<sup>2</sup> Polymerization initiated by the excited nanoparticles, which is called photocatalytic polymerization,<sup>3,4</sup> not only endues the semiconductor photocatalysis with a new function but also provides a strategy to fabricate the composites of polymers and inorganic nanoparticles. Since the nanoparticles are retained during the photocatalytic polymerization, the polymers and the composites can be obtained simultaneously. It is apparent that the photocatalytic polymerization offers a simplified process to prepare the polymer/inorganic nanocomposites. This method has a promising future

in fabricating photo-cured films, heterojunction composites, and protective coatings on semiconductors. Considering that lots of semiconductor nanoparticles are able to perform photocatalysis under the irradiation of visible-light,<sup>5</sup> one can take advantage of solar energy to produce the nanocomposites. In addition, utilization of the photocatalytic polymerization can greatly improve the problem of slow solidification rates for water-borne building coatings.

Poly(methyl methacrylate) (PMMA) is well known for its high transparence and predominant optical homogeneity. Besides applied in the copolymerization to synthesize various plastics and coatings, PMMA can find high valuable applications in photoelectric elements and UV microlithography due to its optical properties.<sup>6</sup> As semiconductor nanoparticles are characterized by their photoelectric properties, it is believed that new photoelectric devices can be assembled by means of incorporating semiconductor inorganic nanoparticles with PMMA. Several research groups have dealt with PMMA on the surface of metal, silicon and aluminum oxide. The results indicated that the interfacial structures were determined by the surface microstructures of the substrates, the tacticity of PMMA and the solvents employed in the preparation of PMMA.<sup>6–8</sup> In the case of photocatalytic polymerization, the interface between the resulting polymers and the nanopar-

Correspondence to: X. Ni (xyni@fudan.edu.cn).

Contract grant sponsor: National Nature Science Fund (NSF) of China; contract grant number: 20574011.

ticles is especially attractive since the nanoparticles play a role as reactive initiators. In a previous work,<sup>3</sup> we have reported that in the polymer/inorganic nanocomposites prepared by means of the photocatalytic polymerization, the polymer component displays unique properties including two glass-transition temperatures and enhanced thermal stability. However, the interfacial structure remains puzzling at present.

PMMA chains have two stereoregularity states, i.e. isotactic and syndiotactic. The tacticity of the polymer depends on the route of synthesis. FTIR absorption bands lying in the region from 1500 to 1300 cm<sup>-1</sup> are attributed to asymmetrical vibrations of CH<sub>3</sub> in forms of methoxyl (O—CH<sub>3</sub>) and α—CH<sub>3</sub>.<sup>9</sup> The complex bands series in the region of 1100–1300 cm<sup>-1</sup> are due to the ν(C—O) stretching coupled with skeletal vibration ν<sub>as</sub>(C—C—O).<sup>10</sup> Importantly, these bands are found to be sensitive to the backbone and side-chains conformations of PMMA.<sup>11</sup> For the reasons mentioned above, the absorption region of 1100–1300 cm<sup>-1</sup> has attracted a lot of attention up to now. O'Reilly and coworkers have established an accurate model to calculate conformational energies for different stereoisomers of PMMA, according to the band intensities in this region.<sup>9</sup> As a result, through investigating these bands of PMMA, conformational changes due to intermolecular interactions can be drawn.<sup>12</sup>

In this study, the composites of PMMA and TiO<sub>2</sub> nanoparticles are prepared through the photocatalytic polymerization. In order to make clear the interfacial structure, the composites are investigated by FTIR and XPS analysis.

## EXPERIMENTAL

### Materials

The nanoscale TiO<sub>2</sub> powders used in the experiment were Degussa P25 (containing 80% anatase and 20% rutile) with an average diameter of 21 nm. The other chemicals were of analytical reagent grade. MMA and methanol were distilled before use. Cupric sulfate (A.R.) and acetone (A.R.) were used as received without further purification. Deionized water was employed.

### Polymerization and separation

The TiO<sub>2</sub> powders were dispersed in 120 mL aqueous solution of MMA monomers by the ultrasonic dispersion technique. The single concentration of TiO<sub>2</sub> studied here was 1 g/L. For the interfacial study, the concentration of MMA monomers was 11.4 g/L. After mixed with MMA solution, the aqueous suspension without pH control was poured into

a quartz reactor which was equipped with a magnetic stirrer and a water jacket connected to a circulator of CuSO<sub>4</sub> solution. UV irradiation was carried out by a mercury vapor lamp with two characteristic chief emission peaks at 254 and 365 nm, respectively. The monomers were prevented from the irradiation of 254 nm rays due to the shielding of CuSO<sub>4</sub> solution, and for this reason self-polymerization was avoided.<sup>13</sup> The reactor was sealed properly. The UV irradiation lasted 5 h. The products were obtained by centrifugation the reacted mixture, then washed by water, and at last dried under vacuum to remove traces of monomers. Acetone was employed to dissolve PMMA in the composites, then the residual particles were removed by ultracentrifugation from the solution. The process was repeated three times. All the samples obtained were dried under vacuum for 24 h prior to instrumental analysis. The overall PMMA yield is 85.4% determined by the data of thermogravimetry analysis (TGA).

### Characterization

TEM photographs of the composites were recorded on a Hitachi H-600 microscope. <sup>13</sup>C NMR spectra were recorded on a Bruker DMX500 spectrometer at 300 K using CDCl<sub>3</sub> as solvent. Polymer molecular weights (MW) were determined by GPC (HP Agilent 1100) with THF as solvent and calibrated by standard polystyrene. FTIR spectra were obtained from Mangna IR550 spectrometer by the KBr technique. XPS experiments were carried out on a PHI-5000C ESCA system (Perkin Elmer) with Al Kα radiation (*hν* = 1486.6 eV). Binding energies were calibrated by the containment carbon (C1s = 284.6 eV). The data analysis was carried out by the PHI-MATLAB software provided by PHI Corporation.

## RESULTS AND DISCUSSION

### Interaction between PMMA and TiO<sub>2</sub> inorganic nanoparticles

Figure 1 shows the typical morphology of the composites obtained by the photocatalytic polymerization. It is found that clusters of the nanoparticles are embedded in the polymer matrix [Fig. 1(A)]. The interface of the composites is so compact that no measurable clearance is observed in the high-resolution photograph [Fig. 1(B)]. FTIR analysis demonstrates that the remanent particles after the purification still contain polymers. So two kinds of samples are obtained. One is the polymer bound to the TiO<sub>2</sub> particles (bound PMMA). The other is the pure polymer extracted from the composites (extracted PMMA). Figure 2 shows the <sup>13</sup>C NMR spectrum of the extracted PMMA. The peaks at the chemical shift

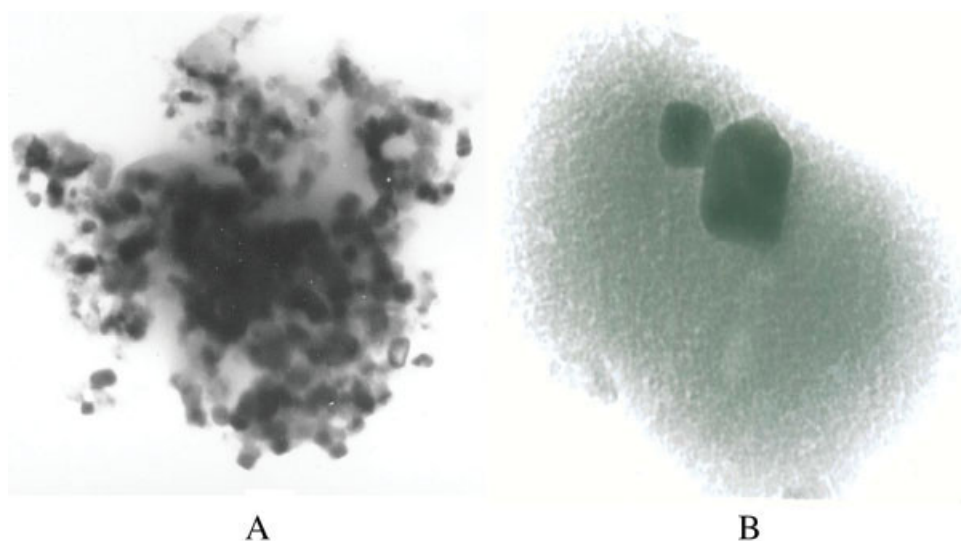


**Figure 1** TEM photographs of the PMMA/TiO<sub>2</sub> composite observed at magnification of  $5 \times 10^3$  (A) and  $1.9 \times 10^5$  (B). [Color figure can be viewed in the online issue, which is available at [www.interscience.wiley.com](http://www.interscience.wiley.com)].

of 44.5 and 51.7 ppm belong to the two backbone carbons, respectively.<sup>14</sup> The split peaks at the chemical shift of 16.5, 18.9, and 21.2 ppm are, respectively, assigned to  $\alpha$ -CH<sub>3</sub> in three kinds of distinct triad sequences, i.e. syndiotactic (rr), heterotactic (mr/rr) and isotactic (mr) sequences.<sup>14</sup> The peaks at 54.4 and 178.0 ppm are attributed to the methoxyl (CH<sub>3</sub>O) and carbonyl (C=O), respectively.<sup>14</sup> Meanwhile it is measured that  $\bar{M}_n$  of the polymer increases from  $4.62 \times 10^4$  to  $8.58 \times 10^4$  while MMA concentration increasing from 7.7 to 11.4 g/L. The above results confirm the synthesis of PMMA. Hence, it is concluded that the photocatalytic polymerization is really a feasible approach to fabricate the composites. Figure 3 shows the FTIR spectral region of 1100–1500 cm<sup>-1</sup> and the carbonyl stretching at ca. 1730 cm<sup>-1</sup> obtained for the two samples. For purpose of comparison, the spectrum of a reference PMMA synthesized using AIBN initiator is also provided in this figure.

The comparison shows that the FTIR spectrum of the extracted PMMA is almost identical to that of the AIBN-initiated PMMA. However, the absorption bands of the bound PMMA differ from the other two obviously. The bands and assignments are tabulated in Table I.<sup>8,9</sup> It is found in Figure 3(A) that the shape of the carbonyl stretching band turns asymmetric with shoulders on the low frequency side, indicating interactions between TiO<sub>2</sub> and the carbonyl groups of PMMA. To understand this variation better, the carbonyl band is resolved and lined in Figure 4. It is seen apparently from the figure that the carbonyl band actually splits into three components at 1730, 1710 and 1694 cm<sup>-1</sup>, respectively. In literature pertaining to PMMA polymers on the metal such as gold, a peak at 1710 cm<sup>-1</sup> was

detected and assigned to the carbonyl bound to the substrates. At the same time a peak due to free carbonyl stretching was found at 1730 cm<sup>-1</sup>.<sup>6,12</sup> In addition to the two similar peaks detected in our PMMA/TiO<sub>2</sub> composites, the peak at 1694 cm<sup>-1</sup> indicates that the interfacial interactions are relatively complex. Several contributors have reported that the peak at this position appears when the carbonyl of PMMA interacts with hydroxyl-containing polymer.<sup>15</sup> Considering the surface hydroxyl of TiO<sub>2</sub> inorganic nanoparticles in the form of >TiOH,<sup>16,17</sup> which will be shown in the following XPS spectra, we believe that our composites have hydrogen bonding between TiO<sub>2</sub> and PMMA. Based on the area of the nonassociated and associated carbonyl stretching peaks in the FTIR spectrum, it is calculated out that

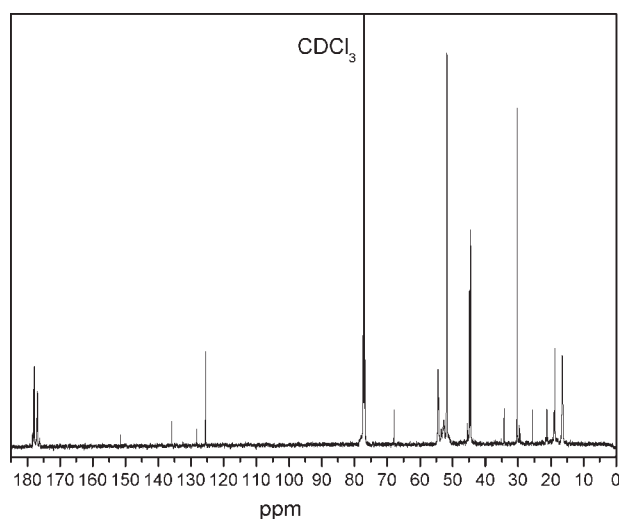


**Figure 2** <sup>13</sup>C NMR spectrum of the PMMA extracted from the composite.

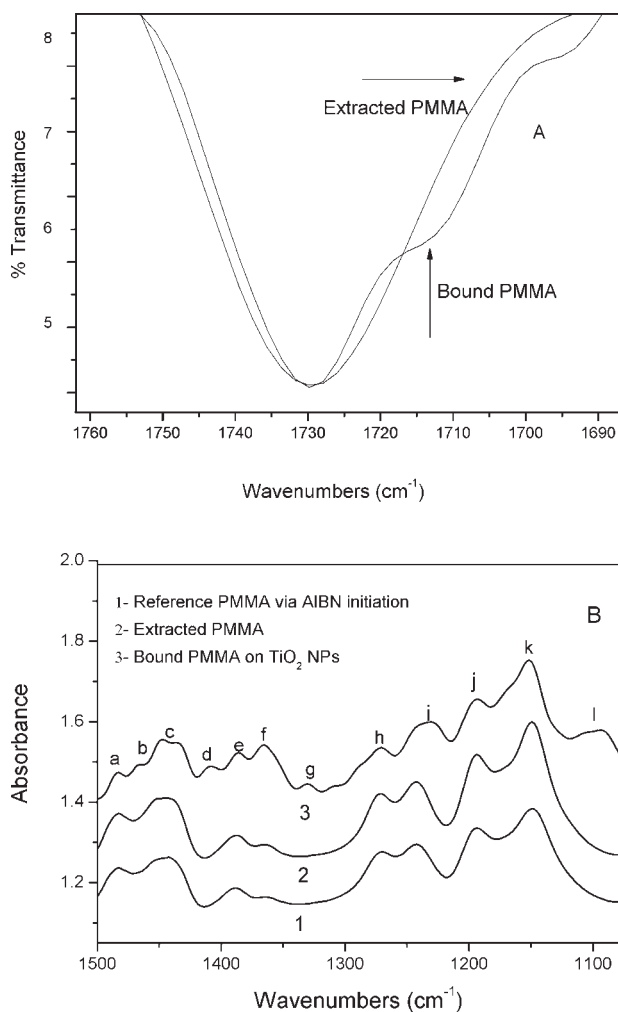


**Figure 3** FTIR spectra of the carbonyl stretching (A) and the range of interest (B).

**TABLE I**  
Assignments of FTIR Peaks (cm<sup>-1</sup>)

Peaks	Frequency, cm <sup>-1</sup>		Assignments
	1 and 2	3	
a	1483	1483	α-CH <sub>3</sub> bending
b		1469	carboxylate asymmetric stretching
c	1448	split	CH <sub>2</sub> bending coupled with CH <sub>3</sub> -O bending
d		1409	Carboxylate symmetric stretching
e	1388	1387	α-CH <sub>3</sub> bending
f	1364	1366	α-CH <sub>3</sub> bending
g		1330	C <sup>α</sup> -C-O stretching vibration
h	1272	1272	C-C-O stretching coupled with C-O stretch
i	1242	1235	C-C-O stretch coupled with C-O stretching
j	1193	1193	C-H deformations
k	1148	1151	C-H deformations
l		1091	Ti-O-C stretching

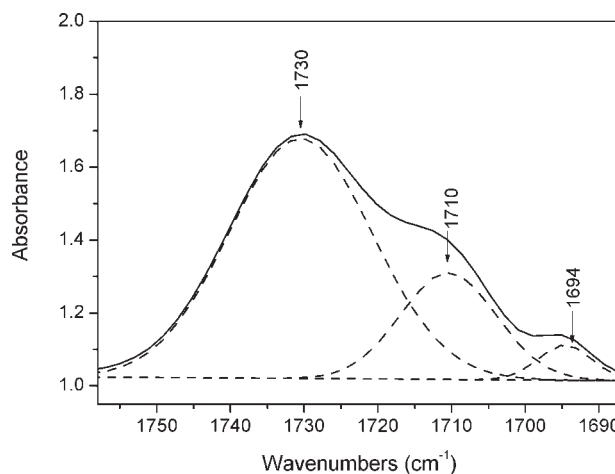


**Figure 4** Splitting of the carbonyl stretching observed for the bound PMMA.

the bound PMMA is constituted of 70% repeating units in nonassociated state and 30% units associated to TiO<sub>2</sub> inorganic nanoparticles.

#### The role of the Ti<sup>4+</sup> cations

To examine the role of Ti<sup>4+</sup> in the interfacial interactions, we compare the Ti 2p XPS spectrum of the composites with that of neat TiO<sub>2</sub>, as shown in Figure 5. In the case of neat TiO<sub>2</sub>, the Ti 2p<sub>1/2</sub> and Ti 2p<sub>3/2</sub> photoelectron peaks are located at the binding energies of 464.7 and 459.0 eV, respectively, which are the typical values for the Ti<sup>4+</sup> cation.<sup>5,18</sup> As for the composite, the Ti 2p doublet is found to shift to lower binding energy by 1.0 eV. The downshift in the binding energy of Ti 2p orbit means that the electron density around the Ti<sup>4+</sup> cation has increased.<sup>19</sup> Such phenomenon is usually detected when the Ti<sup>4+</sup> cation is bound to electron donors. For instance, a downshift of 0.8 eV in the Ti 2p bind-

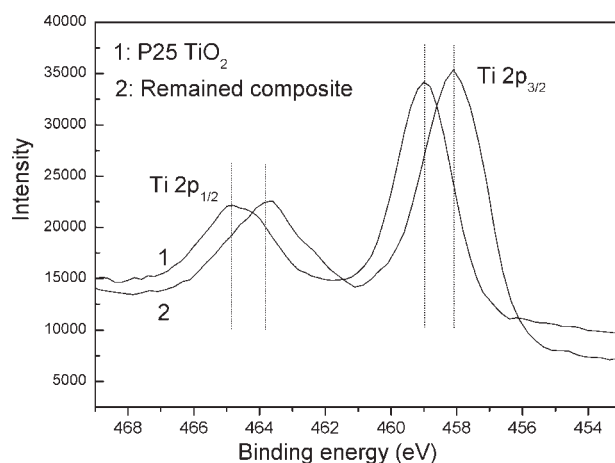


**Figure 5** XPS spectra of Ti 2p orbits for the neat TiO<sub>2</sub> and the composites.



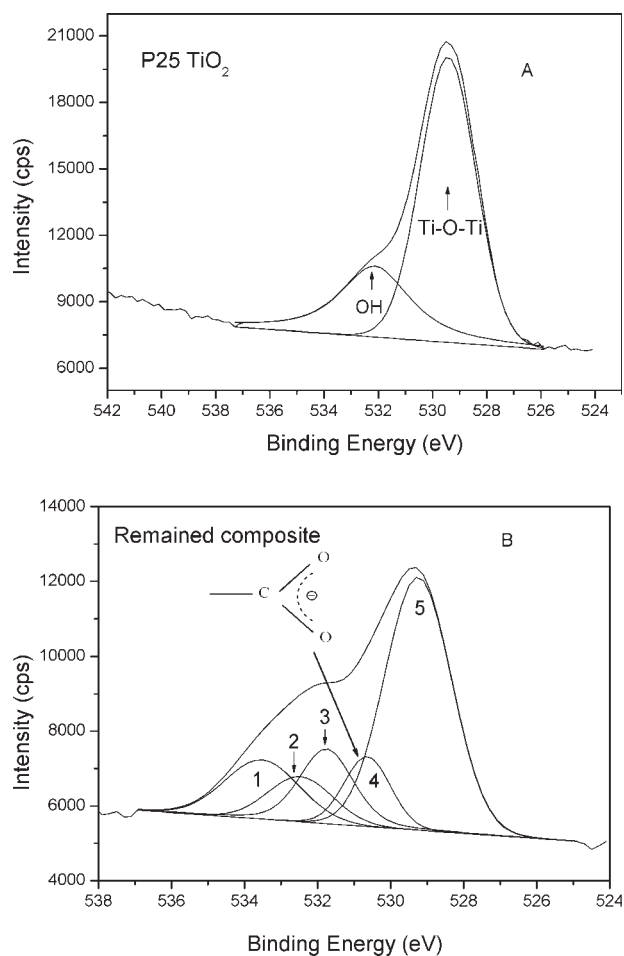


**Figure 6** XPS spectra of O 1s for the neat TiO<sub>2</sub> (A) and the composites (B).

ing energy was measured for the N-doped TiO<sub>2</sub> due to the >Ti–N linkage.<sup>19</sup> The downshift detected here reveals that the Ti<sup>4+</sup> cation interacts with PMMA. As a result, we can assign the FTIR peak at 1710 cm<sup>-1</sup> to the bonding between the carbonyl of PMMA and the Ti<sup>4+</sup> of TiO<sub>2</sub>.

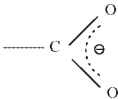
Figure 6 shows the high-resolution XPS spectra of O 1s obtained for neat TiO<sub>2</sub> and the composite. The spectrum of neat TiO<sub>2</sub> is fitted by two components with the same FWHM (full-width at half maximum) of 2.5 eV. The major component at the binding energy of 529.4 eV is assigned to bulk oxide of TiO<sub>2</sub> (O<sup>2-</sup>), while the component at 532.1 eV is assigned to

the surface hydroxyl (>TiOH).<sup>16,17</sup> As for the composite, three peaks at 533.5 eV (peak 2), 531.8 eV (peak 1) and 530.6 eV (peak 4) appear in addition to the inherent peaks of neat TiO<sub>2</sub>. Binding energies and assignments for all the components are shown in Table II. We assign the peak at 533.5 eV to carboxyl oxygen and the peak at 531.8 eV to carbonyl oxygen, since the binding energies detected are typical values for the oxygen atoms in free PMMA.<sup>20</sup> The additional peak at 530.6 eV is assigned to the two-anchoring carboxylate ring,<sup>8</sup> in which electron is delocalized. This result indicates that both carboxyl and carbonyl in PMMA are engaged in the interaction with TiO<sub>2</sub>. Back to Figure 3, two bands at 1469 and 1409 cm<sup>-1</sup> are attributed to symmetric ( $\nu_s$ ) and asymmetric ( $\nu_{as}$ ) stretching of carboxylate, respectively. This observation agrees with the XPS analysis very well.

### Conformation of the bound polymers

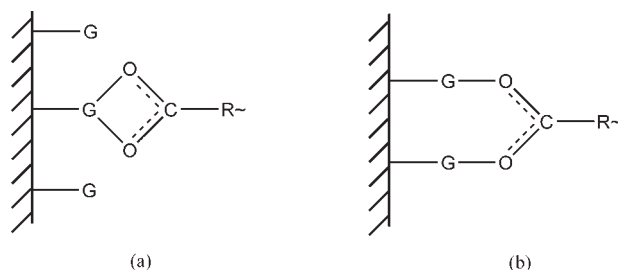
Scheme 1 illustrates two possible complex structures for the PMMA bound on TiO<sub>2</sub>, i.e. the two oxygen atoms of PMMA are linked to two reactive centers or sole reactive center on the TiO<sub>2</sub> surface. They give rise to the bridging complex and the bidentate complex, respectively. It is important to realize in this discussion that the splitting of the carboxylate stretching,  $\Delta(\nu_{as} - \nu_s)$ , enables us to distinguish the complex structures from each other.<sup>21</sup> Tackett<sup>22</sup> has proposed an empirical rule to describe the relationship between the complex structures and  $\Delta(\nu_{as} - \nu_s)$ , which is summarized as follows: bridging (140–170 cm<sup>-1</sup>), bidentate (40–80 cm<sup>-1</sup>), unidentate (200–300 cm<sup>-1</sup>). Nara et al.<sup>23</sup> have demonstrated that this order is related to the changes in bond lengths and angles of the complexes. As the value of  $\Delta(\nu_{as} - \nu_s)$  is equal to 60 cm<sup>-1</sup> here, it is deduced that the composites of PMMA/TiO<sub>2</sub> adopt the bidentate structure. Moreover considering the binary functions of the >Ti<sup>4+</sup>OH group, the formation of bidentate structure is reasonable. It is known that the Ti<sup>4+</sup> with empty 3D orbitals intends to coordinate with the atoms owning electron pairs, such as  $\pi$  electrons of carbonyl oxygen and the sole electron pairs of carboxyl oxygen. Meanwhile the –OH group can interact with polymers through hydrogen bonding.

**TABLE II**  
Binding Energies of the Components in O 1s XPS Spectra

O 1s peaks	1	2	3	4	5
	C=O	C–O–C	OH		Ti–O–Ti
P25 TiO <sub>2</sub> (eV)			532.1		529.4
The remained composite (eV)	531.8	533.5	532.5	530.6	529.3

Therefore we believe that in the composite, the Ti<sup>4+</sup> and —OH of >Ti<sup>4+</sup>OH are linked to different atoms of PMMA. Such a structure is equivalent to the bidentate complex in terms of bond length and angle. In conclusion, the bidentate structure results from the binary functions of the >Ti<sup>4+</sup>OH group.

In the following, we discuss the changes in chain conformation as a result of the surface bonding. According to the method reported by lots of researchers,<sup>24</sup> the IR bands in the 1100–1300 cm<sup>-1</sup> range are fitted into four peaks, as shown in Figure 7. We find that the ratio of A(v<sub>2</sub>)/A(v<sub>1</sub>) for the bound PMMA (2.29) is higher than that of the extracted PMMA (1.79). In 1966, Havriliak and Roman<sup>25</sup> reported that the pair of v<sub>1</sub>, v<sub>2</sub> peaks are associated with two rotational-isomeric states, in which the C=O and α—CH<sub>3</sub> groups are in mutual cis or trans orientation. Furthermore, other contributors demonstrated that the ratio of integrated intensities for the two peaks is related to the difference in conformational energies between *tt* (trans to trans) and *tg* (trans to gauche) conformation in the Newman projection.<sup>12</sup> According to the model established by O'Reilly and Mosher,<sup>9</sup> the intensity of v<sub>1</sub> peak is associated with the conformational energy of the whole chain segment, ΔE<sub>bb</sub> + ΔE<sub>sc</sub>, where ΔE<sub>bb</sub> and ΔE<sub>sc</sub> refers to the backbone conformational energy and the side-chain conformational energy, respectively. The intensity of v<sub>2</sub> peak is associated with ΔE<sub>bb</sub>. The calculations on FTIR and NMR data about s-PMMA, a-PMMA and i-PMMA revealed that the s-PMMA has the largest ratio of A(v<sub>2</sub>)/A(v<sub>1</sub>).<sup>9</sup> Meanwhile the appearance probability of the trans conformation actually increases with the ratio of syndiotacticity.<sup>9</sup> The implication to us is that the backbone chains of the bound PMMA on the TiO<sub>2</sub> surface have to change their rotational conformations from gauche to trans, in contrast to the extracted PMMA. It has been drawn earlier in this article that 30% units of the bound PMMA are bound to the TiO<sub>2</sub> surface. As a result, it is deduced that the polymer covering the surface of the nanoparticles have taken a sheet configuration.



**Scheme 1** Schematic diagram of the binding modes proposed for PMMA/TiO<sub>2</sub> nanocomposites: (a) the bidentate structure and (b) the bridging structure. The symbol of G refers to the >TiOH group of TiO<sub>2</sub> inorganic nanoparticles.

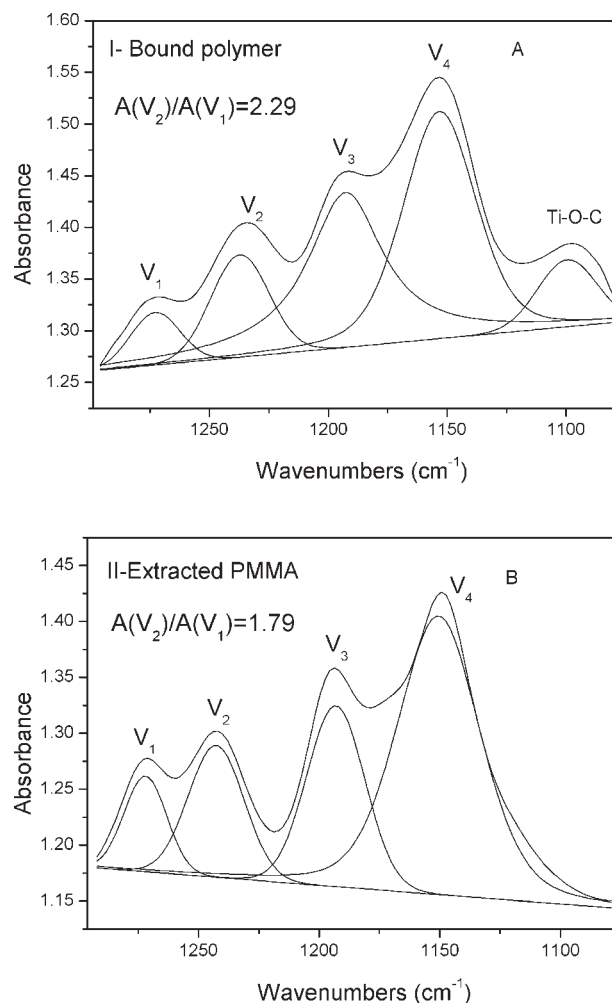


**Figure 7** High-resolution FTIR spectra in the range of 1000–1300 cm<sup>-1</sup>. (A) The bound PMMA and (B) the extracted PMMA.

We believe that the polymerization will not take place until the monomers noticeably, even saturatedly absorb on the surface of TiO<sub>2</sub>. First, the MMA monomers are absorbed to form a liquid layer, then the TiO<sub>2</sub> inorganic nanoparticles under UV irradiation initiate the so-called in-situ polymerization on the surface, leading to the compact interfacial structure as shown in Figure 1. The extracted PMMA that can be isolated from the composite is interpreted in terms of the chain transfer reaction. On the contrary, if polymerization was instantly initiated once monomers reached the surface of bare TiO<sub>2</sub> particles, a brush-like configuration would form and the chains would extend from the surface just like the teeth of a brush.

## CONCLUSIONS

The composites of PMMA and TiO<sub>2</sub> inorganic nanoparticles with compact interface were prepared by

the photocatalytic polymerization. The bound PMMA was found to display triply split IR bands in the carbonyl stretching and change greatly in the range closely related to the conformation of PMMA. It was calculated out that the bound PMMA consisted of 70% repeating units in the nonassociated state and 30% units engaged in the interaction. XPS results showed that the Ti 2p doublet of the TiO<sub>2</sub> in the composite shifts to lower binding energy by 1.0 eV. The bidentate complex with both carboxyl and carbonyl engaged in the interaction was established for the composite prepared in this study. As to the PMMA bound to the TiO<sub>2</sub> inorganic nanoparticles' surface, certain backbone chains have to change their rotational conformations from gauche to trans to interact with the active centers on the surface of TiO<sub>2</sub> inorganic nanoparticles.

Shanghai Nanotechnology and Science Promotion Center is greatly appreciated. The authors thank Prof. Xinghai Yu, faculty of inorganic material chemistry, Fudan University, for kindly helping in XPS measurements.

## References

1. Caseri, W. R. *Mater Sci Technol* 2006, 22, 807.
2. Hoffman, A. J.; Yee, H.; Mills, G.; Hoffman, M. R. *J Phys Chem* 1992, 96, 5540.
3. Dong, C.; Ni, X. Y. *J Macromol Sci Pure A* 2004, 41, 547.
4. Ni, X. Y.; Ye, J.; Dong, C. *J Photochem Photobiol A: Chem* 2006, 181, 19.
5. Grubert, G.; Stockenhuber, M.; Tkachenko, O. P.; Wark, M. *Chem Mater* 2002, 14, 2458.
6. Steiner, G.; Zimmerer, C.; Salzer, R. *Langmuir* 2006, 22, 4125.
7. Berquier, J. M.; Arribart, H. *Langmuir* 1998, 14, 3716.
8. Konstadinidis, K.; Thakkar, B.; Chakraborty, A.; Potts, L. W.; Tannenbaum, R.; Tirrell, M. *Langmuir* 1992, 8, 1307.
9. O'Reilly, J. M.; Mosher, R. A. *Macromolecules* 1981, 14, 602.
10. Willis, H. A.; Zichy, V. J. I.; Hendra, P. J. *Polymer* 1969, 10, 737.
11. Nagai, H. *J Appl Polym Sci* 1963, 7, 1697.
12. Grohens, Y.; Auger, M.; Prudhomme, R.; Schultz, J. *J Polym Sci Part B: Polym Phys* 1999, 37, 2985.
13. Lu, Z. J.; Huang, X. Y.; Huang, J. L. *J Polym Sci Part A: Polym Chem* 1997, 36, 109.
14. Edzes, H. T. *Polymer* 1983, 24, 1425.
15. Dong, J.; Ozaki, Y. *Macromolecules* 1997, 30, 286.
16. Jensen, H.; Soloviev, A.; Li, Z. S.; Søgaard, E. G. *Appl Surf Sci* 2005, 246, 239.
17. Erdem, B.; Hunsicker, R. A.; Simmons, G. W.; Sudol, E. D.; Dimonie, V. L.; El-Aasser, M. S. *Langmuir* 2001, 17, 2664.
18. Sivalingam, G.; Nagaveni, K.; Hegde, M. S.; Madras, G. *Appl Catal B* 2003, 45, 23.
19. Sathish, M.; Viswanathan, B.; Viswanath, R. P.; Gopinath, C. S. *Chem Mater* 2005, 17, 6349.
20. Wochnowski, C.; Shams Eldin, M. A.; Metev, S. *Polym Degrad Stabil* 2005, 89, 252.
21. Doeuff, S.; Henry, M.; Sanchez, C.; Livage, J. *J Non-Cryst Solids* 1987, 89, 206.
22. Tackett, J. E. *Appl Spectrosc* 1989, 43, 483.
23. Nara, M.; Torii, H.; Tasumi, M. M. *J Phys Chem* 1996, 100, 19812.
24. Tretinnikov, O. N.; Ohta, K. *Macromolecules* 2002, 35, 7343.
25. Havriliak, S.; Roman, N. *Polymer* 1966, 7, 387.